Journal of the European Ceramic Society **12** (1993) 461–466

Y_2O_3–CeO_2-Doped ZrO_2 Ceramics from Coprecipitated Oxalate Precursors

Gerhard Gritzner & Peter Steger

Institut für Chemische Technologie Anorganischer Stoffe, Johannes Kepler Universität Linz, A-4040 Linz, Austria

(Received 14 January 1993; revised version received 3 June 1993; accepted 21 June 1993)

Abstract

Y_2O_3–CeO_2-doped ZrO_2 ceramics were prepared from coprecipitated oxalate precursor material. The thermal decomposition behaviour of the oxalates was studied to find proper conditions for conversion to the oxides. The properties of the calcined oxide powders were measured and sintering conditions to prepare ceramic specimen were investigated. The mechanical properties of the sintered bodies are reported and their relations to composition and sintering conditions will be discussed.

Y_2O_3–CeO_2-dotierte ZrO_2 Keramik wurde aus kogefällten Oxalaten hergestellt. Das thermische Zersetzungsverhalten der Oxalate wurde untersucht, um geeignete Bedingungen für die Umwandlung in die Oxide zu ermitteln. Die Eigenschaften der kalzinierten, oxidischen Pulver wurden gemessen und Sinterbedingungen zur Herstellung keramischer Probekörper untersucht. Die mechanischen Eigenschaften der Sinterkörper werden angeführt, und ihre Abhängigkeit von der Zusammensetzung und den Sinterbedingungen wird diskutiert.

On a préparé des céramiques de ZrO_2 dopé avec Y_2O_3–CeO_2 à partir d'un précurseur d'oxalate précipité simultanément. On a étudié la décomposition thermique des oxalates afin de déterminer les conditions adéquates à la conversion en oxyde. On a caracterisé les poudres d'oxyde calcinées et étudié les conditions de frittage pour l'élaboration de céramiques. On examine les propriétés mécaniques des produits frittés et on discute de lien entre ces propriétés d'une part, la composition et les conditions de frittage d'autre part.

1 Introduction

Ceramic materials based on ZrO_2 are of considerable interest for advanced ceramics due to the excellent strengths and the high resistances to fracture. These outstanding mechanical properties were obtained by doping ZrO_2 with different other oxides. Additions of oxides such as Y_2O_3 and careful control of the grain size in the sintered materials lead to improved mechanical properties. The improvements were attributed to different strengthening mechanisms, such as transformation toughening or to microcrack formation and subsequent crack branching.[1] Y_2O_3-stabilised tetragonal ZrO_2 (Y-TZP) material shows very high bend-strengths. Unfortunately, exposure of this material to moist air in the temperature range of 150–400°C leads to drastic deterioration of the mechanical properties as a result of the phase transformation on the surface and the formation of surface cracks.[2,3] One of the ways studied to maintain the mechanical properties after annealing in moist air was the addition of CeO_2 to Y-TZP.[4] Y_2O_3–CeO_2-doped ZrO_2 also aroused interest because of its electrical properties[5] and the possibility to use this material in magnetohydrodynamic reactors.[6]

Investigations on ceramics containing 3 mol% Y_2O_3 and 2, 5 and 10 mol% CeO_2 as well as on samples with 10 mol% CeO_2 and 0–6 mol% Y_2O_3 and on ZrO_2 codoped with 10 mol% Y_2O_3 and 0–10 mol% CeO_2 have been reported. Ceramic specimens were made from powders obtained either by ball-milling commercially available Y_2O_3-doped ZrO_2 with CeO_2 powders[4,7,8] or by coprecipitation of all three cations as hydroxides from aqueous solutions[9–12] or by subsequent coprecipitation of Y^{3+} and Zr^{4+} as hydroxides and mixing with CeO_2 (Refs 13 and 14) followed by calcination and sintering procedures. Very little information, however, was given on the mechanical properties of such ceramics in these publications. Recently, we investigated the mechanical properties of Y_2O_3–CeO_2-codoped ZrO_2 ceramics, which were made by impregnating commercially available ZrO_2 (Dynazirkon F) with $Y(NO_3)_3$ and $Ce(NO_3)_3$ followed by conversion to the oxides.[15] Although the bend-strengths of these

Journal of the European Ceramic Society 0955-2219/93/$6.00

Y_2O_3–CeO_2-doped ZrO_2 ceramics were noticeably smaller than those for Y_2O_3-doped ZrO_2, no deterioration in the bend-strengths upon hydrothermal ageing was observed.

In this study we investigated the preparation of Y_2O_3–CeO_2-doped ZrO_2 ceramics with 3 mol% Y_2O_3 and 0, 5, 9, 10, 15, 18 as well as 30 mol% CeO_2 from precursor material made by coprecipitation of yttrium, cerium and zirconium as neutral oxalates from methanolic solutions in order to obtain intimate mixing of the respective cations as well as small particles. The sintering behaviour of the calcined powders and the mechanical properties of the ceramic material will be reported and discussed.

2 Experimental

$ZrOCl_2 . 8H_2O$ (Merck, Germany, >99%), $Y(NO_3)_3 . 6H_2O$ (Alfa >99%) and $Ce(NO_3)_3 . 6H_2O$ (Merck, Germany, >98·5%) were dissolved in the respective stoichiometric amounts in methanol. A 10% excess over the calculated stoichiometric amount of oxalic acid ($H_2C_2O_4 . 2H_2O$, Merck, Germany, >99·5%) was dissolved separately in methanol. The calculation for the stoichiometric amount of oxalic acid was based on the precipitation of $Zr(C_2O_4)_2$. The concentrations of the salts and the oxalic acid, respectively, ranged between 0·5 and 1 mol dm^{-3}. Both solutions were simultaneously fed at a rate of 2·5 ml min^{-1} by means of a peristaltic pump into a thermostated reaction vessel, which contained 300 ml of methanol. The slurry was continuously withdrawn from the reaction vessel and fresh methanol was added.

The coprecipitated oxalates were filtered, washed with 100 ml of methanol and dried at 70°C for 12 h. Following grinding in a pestle mill the coprecipitated oxalates were calcined at 600°C for 3 h. The calcined product was then subjected to attrition milling for 3 h with ZrO_2 balls (diameter 2 mm, ratio of powder to balls 1:6) in 1-propanol in an attritor made from high-density polyethylene. Upon separation of the balls by sieving, the suspension of the precursor material was separated from 1-propanol by centrifugation. The powders were dried and isostatically pressed at 900 bar into blocks of 19 mm × 15 mm × 34 mm. These blocks were sintered at 1000°C for 3 h. Specimen of 4·5 mm × 3·5 mm × 32 mm were cut from these blocks and polished on grinding paper. The samples were heated at a rate of 5°C min^{-1} up to 600°C, at 4°C min^{-1} up to 900°C and at 3°C min^{-1} to the final sintering temperatures between 1400°C and 1600°C. The final temperature was kept for three hours, cooling was performed at 3°C min^{-1}. The sintered samples were ground on a diamond wheel and polished to mirror-like surfaces with diamond paste ranging from 6 to 1 μm.

Three-point bend-strengths were measured on a 20 mm span; the load was increased at 12 N s^{-1}, Mean values were calculated from nine to 14 samples depending on the amount of powder available. Vickers hardnesses were measured under loads ranging from 49 to 250 N. K_{Ic} values were measured using the indentation technique[16] according to the following formula:[17] $K_{Ic} = 0{\cdot}0824\, P/c^{3/2}$; K_{Ic} (GPa); P (N); c (μm).

The phase analysis on powders calcined at 1000°C and on the sintered specimen was carried out by X-ray diffraction (Rigaku Geigerflex d/max II, Japan) in the 2θ range from 20 to 80° employing Ni-filtered CuK_α radiation (40 kV and 20 mA). The fracture surfaces were measured between 26 and 33°.

The densities of the sintered bodies were obtained by the Archimedes principle in isooctan (2,2,4-trimethylpentan). The theoretical densities were calculated from the composition and the individual densities (t-ZrO_2: 6·200 g cm^{-1}, Y_2O_3: 5·010 g cm^{-3}, CeO_2: 7·123 g cm^{-3}). The specific surface areas of the calcined attritor-milled powders were measured by BET (Quantasorb, Quantachrome, USA), the particle size distributions by means of a laser particle sizer (Coulter LS 130, USA). Compositions of the sintered ceramics were analysed by X-ray fluorescence (Rigaku, Geigerflex 3064 M, Japan) at 35 kV and 15 mA with a Rh-anode and LiF 100 as analyser crystal. Ce was determined at 2θ of 79·35° (80 s), Y at 48·71° (80 s) and Zr at 22·55° (10 s). The decomposition behaviour of the coprecipitated oxalates was studied by thermogravimetry with heating rates of 10°C min^{-1} (Stanton Redcraft TG 770, UK). Thermogravimetry up to 1500°C on 22 mg powder samples with 10-fold sensitivity expansion was employed to investigate possible weight changes due to the formation of Ce_2O_3 at higher temperatures.

The samples were thermally etched at 1400°C for 30 min, covered with gold and analysed by optical microscopy. Scanning electron microscopy (SEM) pictures were taken on a JSM-6400 SEM (Jeol, Japan).

3 Results

The coprecipitated oxalates were amorphous (Fig. 1). Thermogravimetric studies of the coprecipitated oxalates showed that conversion to the oxides is completed around 650°C. The thermal decomposition behaviour was found to follow the decomposition of the individual oxalates starting with the loss of water, followed by the loss of CO forming the carbonates and then the conversion to the oxides under the loss of CO_2 (Fig. 2). Based on these

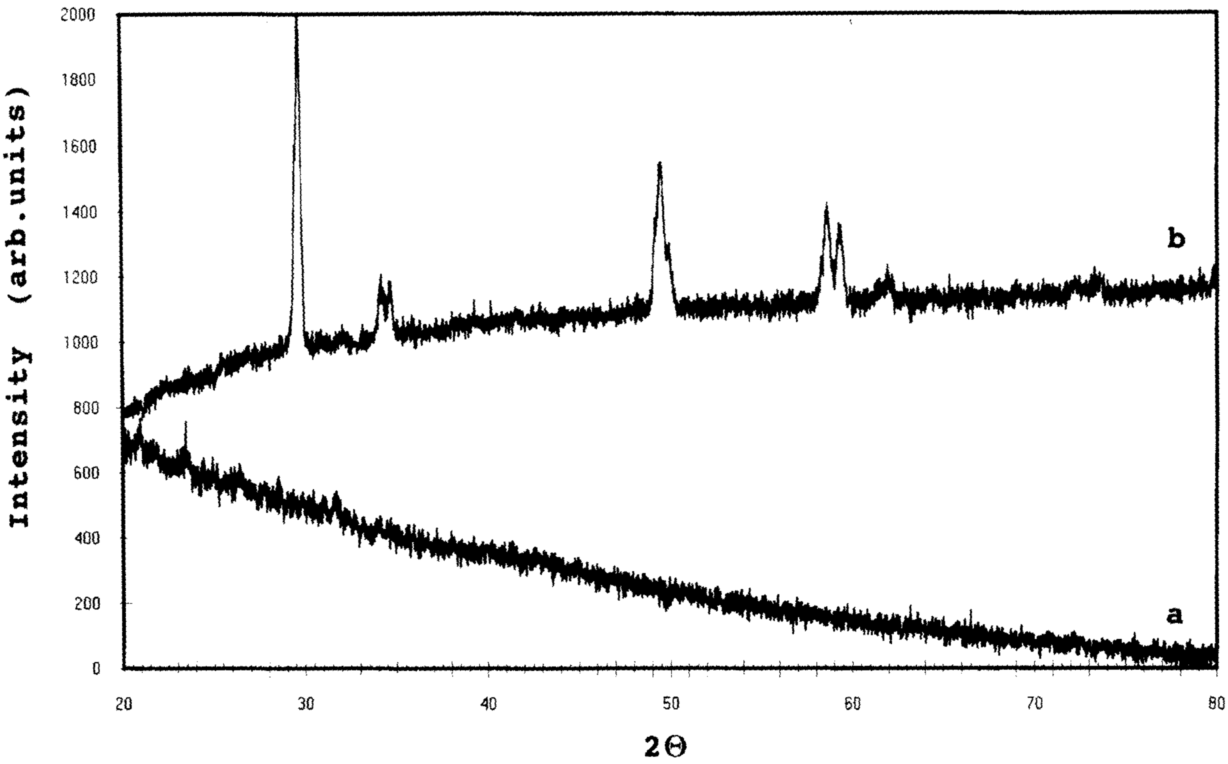

Fig. 1. X-Ray diffraction spectra of (a) coprecipitated oxalates, and (b) the calcined oxides (3 mol% Y_2O_3, 30 mol% CeO_2 and 67 mol% ZrO_2).

observations a calcination temperature of 600°C and a calcination time of 3 h was chosen to assure complete conversion and to limit grain growth during this step.

The calcined powders were dissolved in water and analysed by light-scattering techniques. A bimodal size distribution around 0·3 μm and 6 μm was observed (Fig. 3). N_{50} values of the powders were generally below 0·5 μm. SEM micrographs of the calcined powders showed that the particles consisted of agglomerates of crystallites in the order of 100 nm and smaller (Fig. 4). The specific surface areas of the powders varied between 30 and 39 $m^2 g^{-1}$, the tap densities ranged between 0·65 and 0·70 $g cm^{-3}$. Crystallite sizes (d_{BET}) calculated according to

$$d_{BET} = 6/(\rho S_{BET})$$

where ρ is the theoretical density and S_{BET} is the surface area, ranged between 24 and 32 nm.

X-Ray diffraction measurements of the Y_2O_3–CeO_2 codoped powders with more than 10 mol% CeO_2 and all Y_2O_3–CeO_2 codoped sintered bodies consisted mainly of the tetragonal phase with some cubic phase (Fig. 1). The Y_2O_3-doped powder and the sintered specimen consisted predominantly of tetragonal zirconia with small amounts of mono-

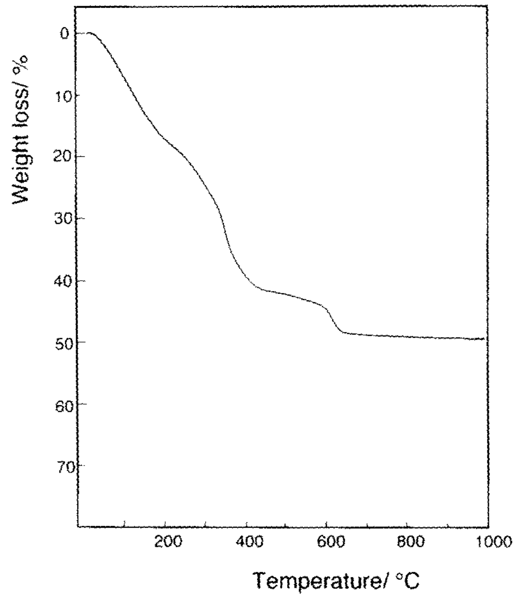

Fig. 2. Thermogravimetry of a coprecipitated oxalate (3 mol% Y_2O_3, 15 mol% CeO_2 and 82 mol% ZrO_2).

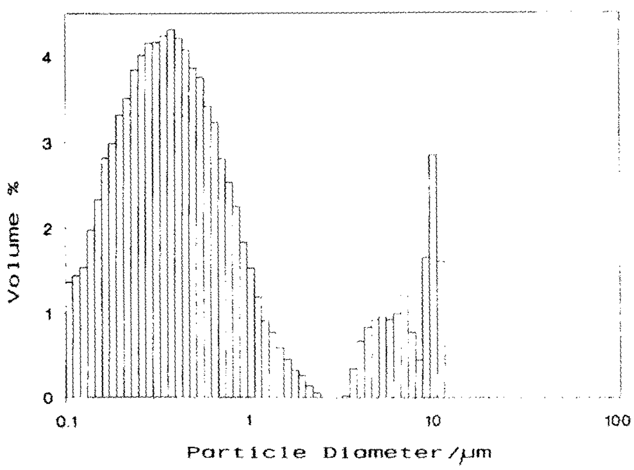

Fig. 3. Particle size distribution of the calcined powder (3 mol% Y_2O_3, 15 mol% CeO_2 and 82 mol% ZrO_2).

Table 1. Mechanical properties of Y_2O_3–CeO_2 doped tetragonal ZrO_2 ceramics

Composition[a] (*mol%*)	*Sinter temperature* (°*C*)	σ_{3P}[b] (*MPa*)	*Weibull modul*	K_{Ic} (*MPa m*$^{1/2}$)	H_v[c] (*GPa*)	ρ[d] (*g cm*$^{-3}$)	*% theoretical density*
3–0	1 400	779	4·5	6·5	12·0	5·90	96·1
	1 500	673	4·0	6·0	11·8	5·92	96·4
	1 600	630	5·1	5·3	10·9	5·81	94·6
3–5	1 400	468	5·1	3·2	11·4	6·03	97·3
	1 500	553	4·5	4·3	11·9	5·94	95·8
	1 600	540	2·9	4·9	11·2	5·88	94·8
3–9	1 400	283	4·4	2·3	11·5	6·22	99·5
	1 500	273	2·9	2·7	11·6	6·15	98·4
	1 600	287	1·6	2·9	10·3	6·14	98·2
3–10	1 400	340	3·9	2·7	12·1	6·08	97·1
	1 500	444	3·1	3·2	11·9	6·08	97·1
	1 600	341	2·6	3·8	11·5	5·97	95·4
3–15	1 400	272	6·7	2·2	11·5	6·25	99·1
	1 500	468	5·3	3·1	12·6	6·14	97·3
	1 600	458	4·0	4·8	11·3	6·13	97·2
3–18	1 500	397	5·1	2·8	11·9	6·15	97·0
	1 600	320	3·8	3·8	10·6	6·08	95·9
3–30	1 400	339	3·7	2·8	12·7	6·26	96·9
	1 500	342	3·0	3·9	13·2	6·13	94·9
	1 600	421	4·0	4·2	12·0	6·09	94·3

[a] Y_2O_3–CeO_2.
[b] Mean three-point bend-strengths.
[c] Vickers hardness.
[d] Density.

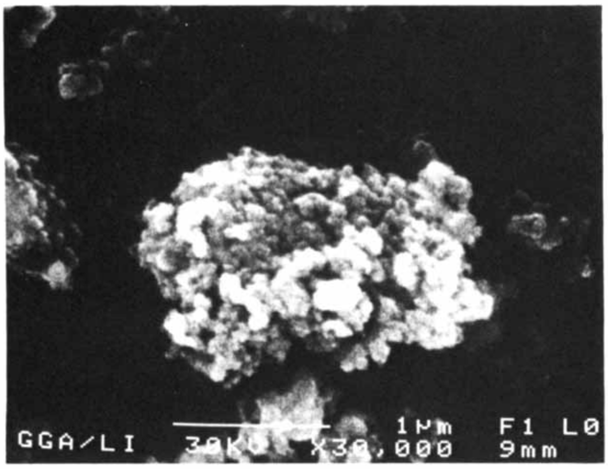

Fig. 4. Scanning electron micrograph of a calcined powder (3 mol% Y_2O_3, 15 mol% CeO_2 and 82 mol% ZrO_2).

clinic phase. The Y_2O_3–CeO_2-codoped powders with 5 mol% CeO_2 were tetragonal. No monoclinic phase was observed on the fracture surfaces of the Y_2O_3–CeO_2-codoped sintered bodies. The mechanical properties of the sintered bodies as a function of the composition and the sintering temperature are summarised in Table 1. The linear shrinkage during sintering was between 22 and 29%.

4 Discussion

Additions of CeO_2 to Y_2O_3-doped ZrO_2 ceramics led to a considerable decrease in the three-point bend-strengths and in the K_{Ic} values compared to samples doped only with Y_2O_3. Although there is considerable scatter in the data for the bend-strengths and the K_{Ic} values, it appears that there is a minimum in the values around 10 mol% CeO_2. Best values for codoped zirconia of 550 MPa were found around 3 mol% Y_2O_3 and 5 mol% CeO_2. The main reason for this decrease in the bend-strengths can be attributed to the lack of transformation toughening. The addition of CeO_2 to Y_2O_3-doped zirconia stabilised the tetragonal phase. Stress-induced tetragonal to monoclinic phase changes did not occur during fracture. Complete stabilisation of the tetragonal phase has been reported for zirconia codoped with 3 mol% Y_2O_3 as well as 2, 4, 6 and 8 mol% CeO_2. Annealing for 50 h at 200°C in humid air only resulted in 10% of the monoclinic phase in samples with 2% CeO_2.[8] Samples with higher CeO_2 contents remained tetragonal and did not show any degradation after the ageing treatment.[8,13,15] Slightly diverting reports exist in the literature for zirconia codoped with 2 mol% Y_2O_3 and varying amounts of CeO_2. While one group observed full stabilisation of the tetragonal phase for samples with 2 mol% Y_2O_3 and CeO_2 contents above 12 mol%,[4] another publication claims that zirconia with 2 mol% Y_2O_3 and CeO_2 concentrations above 6 mol% remained tetragonal following hydrothermal annealing.[13]

Although the specimen studied by us differed in the composition from the published samples, the bend-strengths measured by us are higher for concentrations above 8 mol% CeO_2 than the published values for CeO_2-doped tetragonal zirconia with 2 mol% Y_2O_3. Below 8 mol% CeO_2 the literature data show higher bend-strengths for codoped samples with 2 mol% Y_2O_3, due to some transformation toughening forming monoclinic zirconia.[4] The stabilisation of the tetragonal phase, however, prevents the decrease in bend-strengths during low-temperature ageing in humid atmospheres.[4,8,9,15] The published K_{Ic} values are in the range of 5–18 GPa,[4] 5–6 GPa[7] and 7–8 GPa.[8] Vickers hardnesses increased slightly with the CeO_2 concentration and varied between 10·3 and 13·2 GPa comparable to published data of about 12 GPa for zirconia with 3 mol% Y_2O_3 and 0, 2, 4, 6 and 8 mol% CeO_2, respectively.[8]

Relative densities of the sintered bodies were above 94% and showed a maximum around 10% CeO_2. The highest relative densities were found for specimen sintered at 1400°C. The densities decreased with increasing sintering temperatures. This decrease in the densities with increasing temperature and sintering times was observed before.[9] The following explanation was offered based on SEM micrographs: *intra*- and *inter*-agglomerates are assumed to show different sintering behaviour. At the early stages of sintering the *intra*-agglomerates shrink much faster, but as the sintering time increases pores on the grain boundaries gradually join at grain corners. In a later stage of sintering, the densified agglomerates pull away from neighbouring agglomerates, protrude above the specimen's surface, leaving large voids inside the samples. This explanation is supported by the observed increase in the growth rate of the crystallites upon addition of CeO_2.[7,12] SEM (Fig. 5) and high-resolution optical microscopy (Fig. 6) carried out in this study also clearly showed the enhanced grain growth with increasing sintering temperatures. While sintering at 1400°C yielded grain sizes comparable to the grain size distribution measured for the calcined oxide powders, sintering at 1600°C led to grain sizes up to 5 μm. The large grains amongst many small grains shown in Fig. 6(b) (sintering temperature 1500°C) indicate anisotropic grain growth.

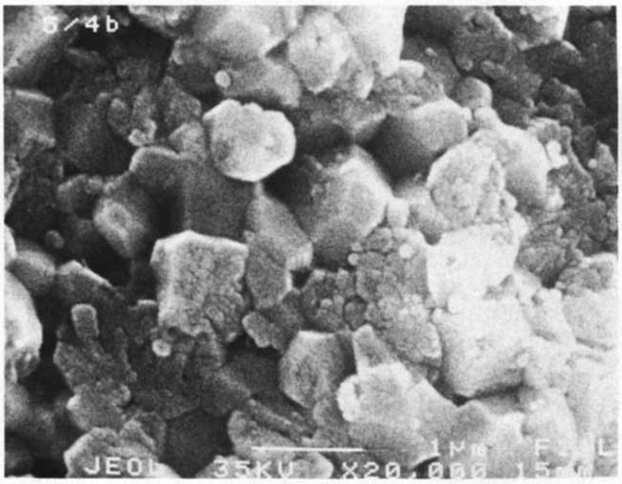

Fig. 5. Scanning electron micrograph of the fracture surface of a specimen (3 mol% Y_2O_3, 10 mol% CeO_2 and 87 mol% ZrO_2) sintered at 1500°C.

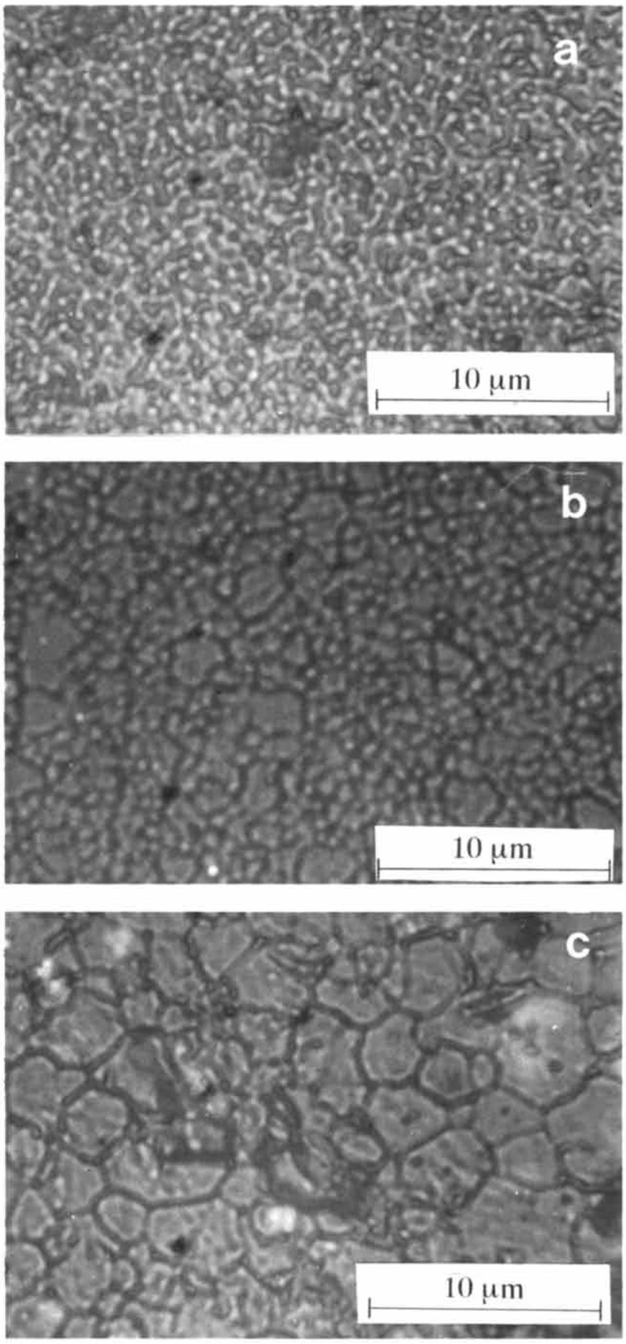

Fig. 6. Optical microscopy of specimen (3 mol% Y_2O_3, 15 mol% CeO_2 and 82 mol% ZrO_2) sintered at (a) 1400°C, (b) 1500°C and (c) 1600°C.

In a recent publication the decrease in the relative densities for Y_2O_3–CeO_2-codoped zirconia was associated with a rapid nucleation of the cubic phase.[15] The reported relative densities for zirconia with 3 mol% Y_2O_3 and 2, 4, 6, 8 and 10% CeO_2 were below 95% even for sintering temperatures between 1300 and 1400°C and dropped to values between 92 and 75% at sintering temperatures of 1600°C.[15] The relative densities measured by us were much better and did not drop below 94% for sintering temperatures of 1600°C. These authors also linked the cubic phase nucleation to the formation of Ce^{3+}, employing diffuse reflectance spectroscopy to estimate the occurrence of Ce^{3+}. Thermogravimetric analysis carried out by us on powders with 3 mol% Y_2O_3 and 0–18 mol% CeO_2 under argon showed only weight losses below 0·015% occurring in the temperature range of 1040°C and 1260°C. No correlation between the Ce content and the weight loss was observed. Therefore, we conclude that reduction to Ce^{3+} cannot account for the observed density changes.

Compared to the Y_2O_3–CeO_2-impregnated zirconia powders studied before[12] we observed bend-strengths improved by 150–200 MPa for the specimen prepared from coprecipitated oxalate precursor material and slightly better Weibull moduli. Vickers hardnesses were comparable. These improvements can be assigned to the small particle size and the intimate mixing of the components in the coprecipitated precursor material.

Acknowledgements

Financial support by the Fonds zur Förderung der wissenschaftlichen Forschung (Österreich) and by the Jubiläumsfonds der Österreichischen Nationalbank is gratefully appreciated. The authors thank Mr K. Kellner for the XRD spectra, Dipl. Ing M. Ratajski for the electron micrographs and Dr P. Diko for his help in the high-resolution optical microscopy.

References

1. Butler, E. P., Transformation-toughened zirconia ceramics. *Mater. Sci. Technol.*, **1** (1985) 417.
2. Claussen, N., Strengthening strategies for ZrO_2-toughened ceramics at high temperatures. *Mater. Sci. Engng*, **71** (1985) 23.
3. Kobayashi, K., Kuwajima, H. & Masaki, T., Phase change and mechanical properties of ZrO_2–Y_2O_3 solid electrolyte after ageing. *Solid State Ion.*, **3–4** (1981) 489.
4. Sato, T., Fukushima, T., Endo, T. & Shimada, M., Thermal stability and mechanical properties of yttria and ceria doped zirconia/alumina composite. *Sci. Ceram.*, **14** (1988) 843.
5. Khan, N., Leach, C. & Steele, B. C. H., Influence of microstructure on the electrical and mechanical behaviour of selected compositions in the Zr–Ce–Y–O system. In *Euro-Ceramics, Vol. 2: Properties of Ceramics*, ed. G. de With, R. A. Terpstra & R. Metselaar. Elsevier Science Publishers, London, UK, 1989, pp. 241–5.
6. Ananthapadmanabhan, P. V., Venkatramani, N., Rohagati, V. K., Momin, A. C. & Vekateswarlu, K. S., Structure and ionic conductivity of solid solutions in the system $0{\cdot}9\{(ZrO_2)_{1-x}$–$(CeO_2)_x\}$–$0{\cdot}1(Y_2O_3)$. *J. Eur. Ceram. Soc.*, **6** (1990) 111.
7. Sato, T., Endo, T. & Shimada, M., Control of the tetragonal to monoclinic phase transformation of yttria doped tetragonal ZrO_2 polycrystals by annealing in water. *Mater. Sci. Res.*, **21C** (1987) 215.
8. Sato, T., Ohtaki, S., Endo, T. & Shimada, M., Improvement of thermal stability of yttria-doped tetragonal zirconia polycrystals by alloying with various oxides. *Int. J. High Technol. Ceram.*, **2** (1986) 167.
9. Duh, J. G. & Lee, M. Y., Fabrication and sinterability in Y_2O_3–CeO_2–ZrO_2. *J. Mater. Sci.*, **24** (1989) 4467.
10. Urabe, K., Ogota, K., Ikawa, H. & Udagawa, S., Phase transformation and lattice constants of zirconia solid solutions in the system Y_2O_3–CeO_2–ZrO_2. In *Ceramic Developments*, ed. C. C. Sorrell & B. Ben-Nissan. Trans. Tech. Publications, Switzerland, 1988, p. 147.
11. Urabe, K., Kakajima, A., Ikawa, H. & Udagawa, S., Characteristic microstructure of CeO_2- and Y_2O_3-doped tetragonal zirconia polycrystals. *Adv. Ceram.*, **24A** (1988) 345.
12. Theunissen, G. S. A. M., Winnubst, A. J. A. & Burggraaf, A. J., Effect of dopants on the sintering behaviour and stability of tetragonal zirconia ceramics. *J. Eur. Ceram. Soc.*, **9** (1992) 251.
13. Hernandez, T., Jurado, J. R. & Duran, P., XPS studies to elucidate the ageing behaviour of Y_2O_3–TZP and Y_2O_3–TZP–CeO_2 ceramics. In *Ceramics Today—Tomorrow's Ceramics*, ed. P. Vincenzini. Elsevier Publisher BV, Amsterdam, The Netherlands, 1991, p. 649.
14. Hernandez, T., Jurado, J. R. & Duran, P., Processing characterization and sintering behaviour of Y_2O_3–TZP and Y_2O_3–TZP–CeO_2 ceramics. In *Ceramics Today—Tomorrow's Ceramics*, ed. P. Vincenzini. Elsevier Publisher BV, Amsterdam, The Netherlands, 1991, p. 1395.
15. Spielbüchler, P. & Gritzner, G., Mechanical properties of yttria and ceria doped zirconia ceramics. *J. Mater. Sci. Lett.*, **11** (1992) 1426.
16. Niihara, K., Morena, R. & Hasseleman, D. P. H., Evaluation of K_{Ic} of brittle solid by the indentation method with low crack-to-indent ratios. *J. Mater. Sci. Lett.*, **1** (1982) 13.
17. Hufenbach, W. & Gerhardy, T., Computer-aided quality assurance of ceric materials and parts by statistical registration of the strength properties. *Radex-Rundschau* (1990) 257.